

Hard Single Diffraction in $\bar{p}p$ Collisions at $\sqrt{s} = 630$ and 1800 GeV

B. Abbott,⁴⁷ M. Abolins,⁴⁴ V. Abramov,¹⁹ B.S. Acharya,¹³ D.L. Adams,⁵⁴ M. Adams,³⁰ S. Ahn,²⁹ V. Akimov,¹⁷ G.A. Alves,² N. Amos,⁴³ E.W. Anderson,³⁶ M.M. Baarmand,⁴⁹ V.V. Babintsev,¹⁹ L. Babukhadia,⁴⁹ A. Baden,⁴⁰ B. Baldin,²⁹ S. Banerjee,¹³ J. Bantly,⁵³ E. Barberis,²² P. Baringer,³⁷ J.F. Bartlett,²⁹ U. Bassler,⁹ A. Belyaev,¹⁸ S.B. Beri,¹¹ G. Bernardi,⁹ I. Bertram,²⁰ V.A. Bezzubov,¹⁹ P.C. Bhat,²⁹ V. Bhatnagar,¹¹ M. Bhattacharjee,⁴⁹ G. Blazey,³¹ S. Blessing,²⁷ A. Boehnlein,²⁹ N.I. Bojko,¹⁹ F. Borchering,²⁹ A. Brandt,⁵⁴ R. Breedon,²³ G. Briskin,⁵³ R. Brock,⁴⁴ G. Brooijmans,²⁹ A. Bross,²⁹ D. Buchholz,³² V. Buescher,⁴⁸ V.S. Burtovoi,¹⁹ J.M. Butler,⁴¹ W. Carvalho,³ D. Casey,⁴⁴ Z. Casilum,⁴⁹ H. Castilla-Valdez,¹⁵ D. Chakraborty,⁴⁹ K.M. Chan,⁴⁸ S.V. Chekulaev,¹⁹ W. Chen,⁴⁹ D.K. Cho,⁴⁸ S. Choi,²⁶ S. Chopra,²⁷ B.C. Choudhary,²⁶ J.H. Christenson,²⁹ M. Chung,³⁰ D. Claes,⁴⁵ A.R. Clark,²² W.G. Cobau,⁴⁰ J. Cochran,²⁶ L. Coney,³⁴ B. Connolly,²⁷ W.E. Cooper,²⁹ D. Coppage,³⁷ D. Cullen-Vidal,⁵³ M.A.C. Cummings,³¹ D. Cutts,⁵³ O.I. Dahl,²² K. Davis,²¹ K. De,⁵⁴ K. Del Signore,⁴³ M. Demarteau,²⁹ D. Denisov,²⁹ S.P. Denisov,¹⁹ H.T. Diehl,²⁹ M. Diesburg,²⁹ G. Di Loreto,⁴⁴ P. Draper,⁵⁴ Y. Ducros,¹⁰ L.V. Dudko,¹⁸ S.R. Dugad,¹³ A. Dyshkant,¹⁹ D. Edmunds,⁴⁴ J. Ellison,²⁶ V.D. Elvira,⁴⁹ R. Engelmann,⁴⁹ S. Eno,⁴⁰ G. Eppley,⁵⁶ P. Ermolov,¹⁸ O.V. Eroshin,¹⁹ J. Estrada,⁴⁸ H. Evans,⁴⁶ V.N. Evdokimov,¹⁹ T. Fahland,²⁵ S. Feher,²⁹ D. Fein,²¹ T. Ferbel,⁴⁸ H.E. Fisk,²⁹ Y. Fisyak,⁵⁰ E. Flattum,²⁹ F. Fleuret,²² M. Fortner,³¹ K.C. Frame,⁴⁴ S. Fuess,²⁹ E. Gallas,²⁹ A.N. Galyaev,¹⁹ P. Gartung,²⁶ V. Gavrillov,¹⁷ R.J. Genik II,²⁰ K. Genser,²⁹ C.E. Gerber,²⁹ Y. Gershtein,⁵³ B. Gibbard,⁵⁰ R. Gilmartin,²⁷ G. Ginther,⁴⁸ B. Gobbi,³² B. Gómez,⁵ G. Gómez,⁴⁰ P.I. Goncharov,¹⁹ J.L. González Solís,¹⁵ H. Gordon,⁵⁰ L.T. Goss,⁵⁵ K. Gounder,²⁶ A. Goussiou,⁴⁹ N. Graf,⁵⁰ P.D. Grannis,⁴⁹ D.R. Green,²⁹ J.A. Green,³⁶ H. Greenlee,²⁹ S. Grinstein,¹ P. Grudberg,²² S. Grünendahl,²⁹ G. Guglielmo,⁵² A. Gupta,¹³ S.N. Gurzhiev,¹⁹ G. Gutierrez,²⁹ P. Gutierrez,⁵² N.J. Hadley,⁴⁰ H. Haggerty,²⁹ S. Hagopian,²⁷ V. Hagopian,²⁷ K.S. Hahn,⁴⁸ R.E. Hall,²⁴ P. Hanlet,⁴² S. Hansen,²⁹ J.M. Hauptman,³⁶ C. Hays,⁴⁶ C. Hebert,³⁷ D. Hedin,³¹ A.P. Heinson,²⁶ U. Heintz,⁴¹ T. Heuring,²⁷ R. Hirosky,³⁰ J.D. Hobbs,⁴⁹ B. Hoeneisen,⁶ J.S. Hoftun,⁵³ F. Hsieh,⁴³ A.S. Ito,²⁹ S.A. Jerger,⁴⁴ R. Jesik,³³ T. Joffe-Minor,³² K. Johns,²¹ M. Johnson,²⁹ A. Jonckheere,²⁹ M. Jones,²⁸ H. Jöstlein,²⁹ S.Y. Jun,³² S. Kahn,⁵⁰ E. Kajfasz,⁸ D. Karmanov,¹⁸ D. Karmgard,³⁴ R. Kehoe,³⁴ S.K. Kim,¹⁴ B. Klima,²⁹ C. Klopfenstein,²³ B. Knuteson,²² W. Ko,²³ J.M. Kohli,¹¹ D. Koltick,³⁵ A.V. Kostritskiy,¹⁹ J. Kotcher,⁵⁰ A.V. Kotwal,⁴⁶ A.V. Kozelov,¹⁹ E.A. Kozlovsky,¹⁹ J. Krane,³⁶ M.R. Krishnaswamy,¹³ S. Krzywdzinski,²⁹ M. Kubantsev,³⁸ S. Kuleshov,¹⁷ Y. Kulik,⁴⁹ S. Kunori,⁴⁰ G. Landsberg,⁵³ A. Leflat,¹⁸ F. Lehner,²⁹ J. Li,⁵⁴ Q.Z. Li,²⁹ J.G.R. Lima,³ D. Lincoln,²⁹ S.L. Linn,²⁷ J. Linnemann,⁴⁴ R. Lipton,²⁹ J.G. Lu,⁴ A. Lucotte,⁴⁹ L. Lueking,²⁹ C. Lundstedt,⁴⁵ A.K.A. Maciel,³¹ R.J. Madaras,²² V. Manankov,¹⁸ S. Mani,²³ H.S. Mao,⁴ R. Markeloff,³¹ T. Marshall,³³ M.I. Martin,²⁹ R.D. Martin,³⁰ K.M. Mauritz,³⁶ B. May,³² A.A. Mayorov,³³ R. McCarthy,⁴⁹ J. McDonald,²⁷ T. McKibben,³⁰ T. McMahan,⁵¹ H.L. Melanson,²⁹ M. Merkin,¹⁸ K.W. Merritt,²⁹ C. Miao,⁵³ H. Miettinen,⁵⁶ A. Mincer,⁴⁷ C.S. Mishra,²⁹ N. Mokhov,²⁹ N.K. Mondal,¹³

H.E. Montgomery,²⁹ M. Mostafa,¹ H. da Motta,² E. Nagy,⁸ F. Nang,²¹ M. Narain,⁴¹
V.S. Narasimham,¹³ H.A. Neal,⁴³ J.P. Negret,⁵ S. Negroni,⁸ D. Norman,⁵⁵ L. Oesch,⁴³
V. Oguri,³ B. Olivier,⁹ N. Oshima,²⁹ D. Owen,⁴⁴ P. Padley,⁵⁶ A. Para,²⁹ N. Parashar,⁴²
R. Partridge,⁵³ N. Parua,⁷ M. Paterno,⁴⁸ A. Patwa,⁴⁹ B. Pawlik,¹⁶ J. Perkins,⁵⁴ M. Peters,²⁸
R. Piegaiia,¹ H. Piekarz,²⁷ Y. Pischalnikov,³⁵ B.G. Pope,⁴⁴ E. Popkov,³⁴ H.B. Prosper,²⁷
S. Protopopescu,⁵⁰ J. Qian,⁴³ P.Z. Quintas,²⁹ R. Raja,²⁹ S. Rajagopalan,⁵⁰ N.W. Reay,³⁸
S. Reucroft,⁴² M. Rijssenbeek,⁴⁹ T. Rockwell,⁴⁴ M. Roco,²⁹ P. Rubinov,³² R. Ruchti,³⁴
J. Rutherford,²¹ A. Santoro,² L. Sawyer,³⁹ R.D. Schamberger,⁴⁹ H. Schellman,³²
A. Schwartzman,¹ J. Sculli,⁴⁷ N. Sen,⁵⁶ E. Shabalina,¹⁸ H.C. Shankar,¹³ R.K. Shivpuri,¹²
D. Shpakov,⁴⁹ M. Shupe,²¹ R.A. Sidwell,³⁸ H. Singh,²⁶ J.B. Singh,¹¹ V. Sirotenko,³¹
P. Slattey,⁴⁸ E. Smith,⁵² R.P. Smith,²⁹ R. Snihur,³² G.R. Snow,⁴⁵ J. Snow,⁵¹ S. Snyder,⁵⁰
J. Solomon,³⁰ X.F. Song,⁴ V. Sorín,¹ M. Sosebee,⁵⁴ N. Sotnikova,¹⁸ M. Souza,²
N.R. Stanton,³⁸ G. Steinbrück,⁴⁶ R.W. Stephens,⁵⁴ M.L. Stevenson,²² F. Stichelbaut,⁵⁰
D. Stoker,²⁵ V. Stolin,¹⁷ D.A. Stoyanova,¹⁹ M. Strauss,⁵² K. Streets,⁴⁷ M. Strovink,²²
L. Stutte,²⁹ A. Sznajder,³ J. Tarazi,²⁵ M. Tartaglia,²⁹ T.L.T. Thomas,³² J. Thompson,⁴⁰
D. Toback,⁴⁰ T.G. Trippe,²² A.S. Turcot,⁴³ P.M. Tuts,⁴⁶ P. van Gemmeren,²⁹ V. Vaniev,¹⁹
N. Varelas,³⁰ A.A. Volkov,¹⁹ A.P. Vorobiev,¹⁹ H.D. Wahl,²⁷ J. Warchol,³⁴ G. Watts,⁵⁷
M. Wayne,³⁴ H. Weerts,⁴⁴ A. White,⁵⁴ J.T. White,⁵⁵ J.A. Wightman,³⁶ S. Willis,³¹
S.J. Wimpenny,²⁶ J.V.D. Wirjawan,⁵⁵ J. Womersley,²⁹ D.R. Wood,⁴² R. Yamada,²⁹
P. Yamin,⁵⁰ T. Yasuda,²⁹ K. Yip,²⁹ S. Youssef,²⁷ J. Yu,²⁹ Y. Yu,¹⁴ M. Zanabria,⁵
H. Zheng,³⁴ Z. Zhou,³⁶ Z.H. Zhu,⁴⁸ M. Zielinski,⁴⁸ D. Zieminska,³³ A. Ziemiński,³³
V. Zutshi,⁴⁸ E.G. Zverev,¹⁸ and A. Zylberstejn¹⁰

(DØ Collaboration)

¹*Universidad de Buenos Aires, Buenos Aires, Argentina*

²*LAFEX, Centro Brasileiro de Pesquisas Físicas, Rio de Janeiro, Brazil*

³*Universidade do Estado do Rio de Janeiro, Rio de Janeiro, Brazil*

⁴*Institute of High Energy Physics, Beijing, People's Republic of China*

⁵*Universidad de los Andes, Bogotá, Colombia*

⁶*Universidad San Francisco de Quito, Quito, Ecuador*

⁷*Institut des Sciences Nucléaires, IN2P3-CNRS, Université de Grenoble 1, Grenoble, France*

⁸*Centre de Physique des Particules de Marseille, IN2P3-CNRS, Marseille, France*

⁹*LPNHE, Universités Paris VI and VII, IN2P3-CNRS, Paris, France*

¹⁰*DAPNIA/Service de Physique des Particules, CEA, Saclay, France*

¹¹*Panjab University, Chandigarh, India*

¹²*Delhi University, Delhi, India*

¹³*Tata Institute of Fundamental Research, Mumbai, India*

¹⁴*Seoul National University, Seoul, Korea*

¹⁵*CINVESTAV, Mexico City, Mexico*

¹⁶*Institute of Nuclear Physics, Kraków, Poland*

¹⁷*Institute for Theoretical and Experimental Physics, Moscow, Russia*

¹⁸*Moscow State University, Moscow, Russia*

¹⁹*Institute for High Energy Physics, Protvino, Russia*

²⁰*Lancaster University, Lancaster, United Kingdom*

- ²¹ *University of Arizona, Tucson, Arizona 85721*
- ²² *Lawrence Berkeley National Laboratory and University of California, Berkeley, California 94720*
- ²³ *University of California, Davis, California 95616*
- ²⁴ *California State University, Fresno, California 93740*
- ²⁵ *University of California, Irvine, California 92697*
- ²⁶ *University of California, Riverside, California 92521*
- ²⁷ *Florida State University, Tallahassee, Florida 32306*
- ²⁸ *University of Hawaii, Honolulu, Hawaii 96822*
- ²⁹ *Fermi National Accelerator Laboratory, Batavia, Illinois 60510*
- ³⁰ *University of Illinois at Chicago, Chicago, Illinois 60607*
- ³¹ *Northern Illinois University, DeKalb, Illinois 60115*
- ³² *Northwestern University, Evanston, Illinois 60208*
- ³³ *Indiana University, Bloomington, Indiana 47405*
- ³⁴ *University of Notre Dame, Notre Dame, Indiana 46556*
- ³⁵ *Purdue University, West Lafayette, Indiana 47907*
- ³⁶ *Iowa State University, Ames, Iowa 50011*
- ³⁷ *University of Kansas, Lawrence, Kansas 66045*
- ³⁸ *Kansas State University, Manhattan, Kansas 66506*
- ³⁹ *Louisiana Tech University, Ruston, Louisiana 71272*
- ⁴⁰ *University of Maryland, College Park, Maryland 20742*
- ⁴¹ *Boston University, Boston, Massachusetts 02215*
- ⁴² *Northeastern University, Boston, Massachusetts 02115*
- ⁴³ *University of Michigan, Ann Arbor, Michigan 48109*
- ⁴⁴ *Michigan State University, East Lansing, Michigan 48824*
- ⁴⁵ *University of Nebraska, Lincoln, Nebraska 68588*
- ⁴⁶ *Columbia University, New York, New York 10027*
- ⁴⁷ *New York University, New York, New York 10003*
- ⁴⁸ *University of Rochester, Rochester, New York 14627*
- ⁴⁹ *State University of New York, Stony Brook, New York 11794*
- ⁵⁰ *Brookhaven National Laboratory, Upton, New York 11973*
- ⁵¹ *Langston University, Langston, Oklahoma 73050*
- ⁵² *University of Oklahoma, Norman, Oklahoma 73019*
- ⁵³ *Brown University, Providence, Rhode Island 02912*
- ⁵⁴ *University of Texas, Arlington, Texas 76019*
- ⁵⁵ *Texas A&M University, College Station, Texas 77843*
- ⁵⁶ *Rice University, Houston, Texas 77005*
- ⁵⁷ *University of Washington, Seattle, Washington 98195*

(November 21, 2018)

Abstract

Using the DØ detector, we have studied events produced in $\bar{p}p$ collisions that contain large forward regions with very little energy deposition (“rapidity gaps”) and concurrent jet production at center-of-mass energies of $\sqrt{s} = 630$ and 1800 GeV. The fractions of forward and central jet events associated with such rapidity gaps are measured and compared to predictions from Monte Carlo models. For hard diffractive candidate events, we use the calorimeter to extract the fractional momentum loss of the scattered protons.

Inelastic diffractive collisions are responsible for 10–15% of the $\bar{p}p$ total cross section and have been described by Regge theory through the exchange of a pomeron [1]. Diffractive events are characterized by the absence of significant hadronic particle activity over a large region of rapidity or pseudorapidity ($\eta = -\ln[\tan(\frac{\theta}{2})]$, where θ is the polar angle relative to the beam). This empty region is called a rapidity gap and can be used as an experimental signature for diffraction. Recent interest in diffraction has centered on the possible partonic nature of the pomeron in the framework of quantum chromodynamics (QCD), as suggested by Ingelman and Schlein [2]. Hard single diffraction (HSD), which combines diffraction and a hard scatter (such as jet or W -boson production), can be used to study the properties of the pomeron.

The partonic nature of the pomeron was first inferred by the UA8 experiment [3] at the CERN $S\bar{p}\bar{p}S$ collider at $\sqrt{s} = 630$ GeV from studies of diffractive jet events. Recent analyses of diffractive jet production [4–6] and diffractive W -boson production [7] are consistent with a predominantly hard gluonic pomeron, but measured rates at the Fermilab Tevatron are several times lower than predictions based on data from the DESY ep collider HERA [8]. In this Letter we present new measurements of the characteristics of diffractive jet events, and of the fraction of central and forward jet events that contain forward rapidity gaps (“gap fraction”) at center-of-mass energies $\sqrt{s} = 630$ and 1800 GeV. These measurements augment previous results from the CDF collaboration on the gap fraction for forward jets at $\sqrt{s} = 1800$ GeV [4] and place further constraints on diffractive models.

In the DØ detector [9], jets are measured using the uranium/liquid-argon calorimeters with an electromagnetic section extending to $|\eta| < 4.1$ and coverage for hadrons to $|\eta| < 5.2$. Jets are reconstructed using a fixed-cone algorithm with radius $\mathcal{R} = \sqrt{\Delta\eta^2 + \Delta\phi^2} = 0.7$ (ϕ is the azimuthal angle). The jets are corrected using standard DØ routines for jet-energy scale [10], except that there is no subtraction of energy from spectator parton interactions, since these are unlikely for diffractive events.

To identify rapidity gaps, we measure the number of tiles containing a signal in the LØ forward scintillator arrays ($n_{LØ}$), and towers ($\Delta\eta \times \Delta\phi = 0.1 \times 0.1$) above threshold in the calorimeters (n_{CAL}). The LØ arrays provide partial coverage in the region $2.3 < |\eta| < 4.3$. A portion of the two forward calorimeters ($3.0 < |\eta| < 5.2$) is used to measure the calorimeter multiplicity, with a particle tagged by the deposition of more than 150 (500) MeV of energy in an electromagnetic (hadronic) calorimeter tower. The thresholds are set to give negligible noise from uranium decays, while maximizing sensitivity to energetic particles [11].

For $\sqrt{s} = 630$ and 1800 GeV, we use triggers which required at least two jets with transverse energy $E_T > 12$ or 15 GeV (see Table I) to study the dependence of the gap fraction on jet location. The forward jet triggers required the two leading jets to both have $\eta > 1.6$ (or $\eta < -1.6$), while the central jet triggers had an offline requirement of $|\eta| < 1.0$. These data were obtained during special low luminosity runs, with typical instantaneous luminosities much less than $1 \times 10^{30} \text{ cm}^{-2}\text{s}^{-1}$. At each \sqrt{s} , we also implemented the so-called single veto trigger (SV), a dijet trigger that required a rapidity gap on one side (using the LØ detector). The SV trigger was used to obtain large samples of single diffractive candidate events. The events in the final data samples all have a single $\bar{p}p$ interaction requirement, a vertex position within 50 cm of the center of the interaction region, and two leading jets that satisfy standard quality criteria [12]. The number of events in each of the final data samples and the integrated luminosities (\mathcal{L}) are given in Table I.

TABLE I. Attributes of the final data samples.

Data Sample	Jet $ \eta $	Jet $E_T(\text{GeV})$	\mathcal{L} (nb^{-1})	Events
1800 GeV Forward	> 1.6	> 12	62.9	50852
1800 GeV Central	< 1.0	> 15	4.55	16567
630 GeV Forward	> 1.6	> 12	16.9	28421
630 GeV Central	< 1.0	> 12	8.06	48123
1800 GeV SV	–	> 15	5700	170393
630 GeV SV	–	> 12	529	64772

The $n_{L\emptyset}$ versus n_{CAL} distributions for central and forward jet events at $\sqrt{s} = 630$ and 1800 GeV are shown in Fig. 1. For forward jet events, these quantities are defined by the η region on the side opposite the two leading jets, while for central jet events they are defined by the forward η interval that has the lower multiplicity. The distributions display a peak at zero multiplicity ($n_{\text{CAL}} = n_{L\emptyset} = 0$), in qualitative agreement with expectations for a diffractive component in the data.

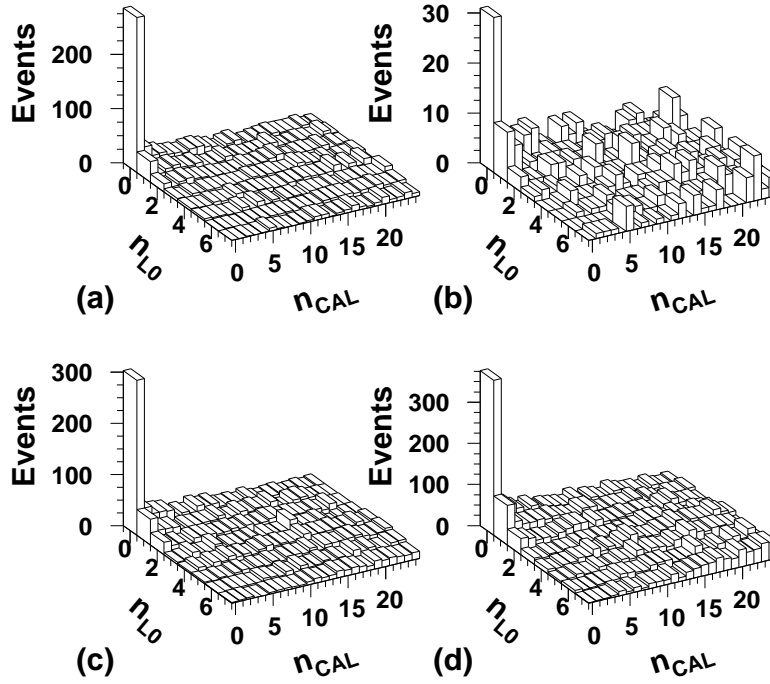


FIG. 1. Multiplicity distributions at $\sqrt{s} = 1800$ GeV for (a) forward and (b) central jet events, and at $\sqrt{s} = 630$ GeV for (c) forward and (d) central jet events.

The gap fraction is extracted from a two-dimensional fit to the lego plot of $n_{L\emptyset}$ versus n_{CAL} . The non-diffractive (high multiplicity) background is fitted in the signal region using a four-parameter polynomial, and the signal is fitted with a falling exponential, as suggested

by Monte Carlo [11]. Figure 2 shows the multiplicity distribution from Fig. 1(a), and the resulting fitted signal, fitted background, and normalized distribution of pulls ($[\text{data-fit}]/\sqrt{N}$). All distributions have adequate fits, with $\chi^2/\text{dof} < 1.2$.

Table II shows the gap fractions obtained for the four event samples. The values range from $(0.22 \pm 0.05)\%$ for central jets at $\sqrt{s} = 1800$ GeV, to $(1.19 \pm 0.08)\%$ for forward jets at $\sqrt{s} = 630$ GeV. Uncertainties are dominated by those on the fit parameters. Additional small uncertainties from the dependence on the range of multiplicity used in the fits were added in quadrature. Potential sources of systematic error, such as the number of fit parameters, jet energy scale, trigger turn-on, tower threshold, luminosity, residual noise, and jet quality, yield only negligible variations in the gap fractions [11].

Table II shows that the gap fractions at $\sqrt{s} = 630$ GeV are larger than gap fractions at $\sqrt{s} = 1800$ GeV and that gap fractions for forward jets are larger than for central jets. Table II also lists predicted gap fractions for several possible pomeron structure functions (discussed below).

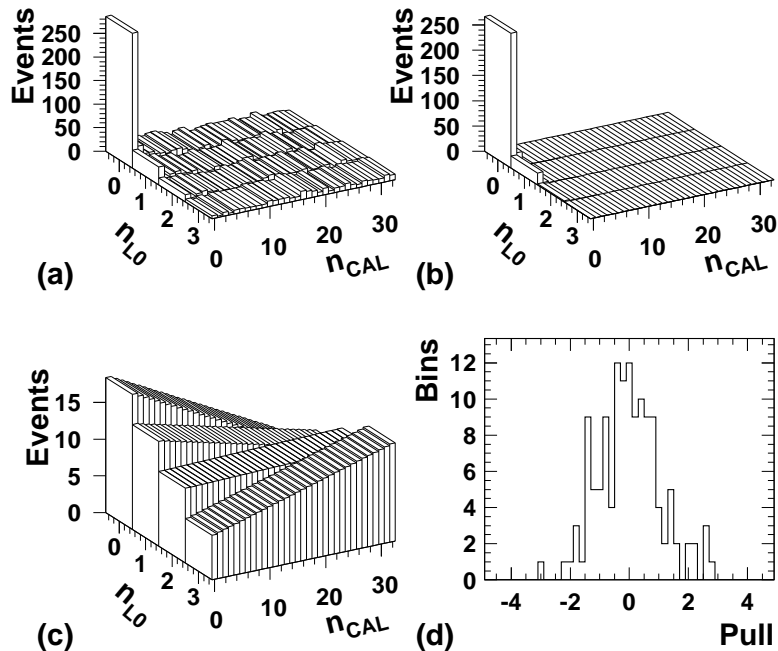


FIG. 2. The (a) data from Fig. 1(a), and corresponding (b) fitted signal, (c) fitted background, and (d) normalized pull distributions.

We compare the data to Monte Carlo (MC) simulations using the hard diffractive event generator POMPYT [13], which is based on the non-diffractive PYTHIA [14] program. In POMPYT, a pomeron is emitted from the proton with a certain probability (called the flux factor [2]), and has a structure functions $s(\beta)$, where β is the fractional momentum of the pomeron carried by the hard parton. We used the standard Donnachie-Lanshoff flux factor [15] in this analysis and compare our data to four structure functions: (i) “hard gluon,” a pomeron consisting of two gluons, $s(\beta) \propto \beta(1 - \beta)$; (ii) “flat gluon,” $s(\beta) \propto \text{constant}$; (iii) “soft gluon,” $s(\beta) \propto (1 - \beta)^5$; and (iv) “quark,” the two-quark analog of (i). In each case, the gap fraction is defined as the cross section for jet events with a rapidity gap based on POMPYT divided by the jet cross section from PYTHIA. Many uncertainties, such as the

choice of proton parton densities, cancel in the ratio. An MC version of the fitting method is applied to correct for diffractive events that fail the gap selection criteria. By applying the appropriate correction factor (which ranges from a few per cent for soft gluon central jets to about 80% for hard gluon forward jets) to each MC prediction and comparing to the data, we make no assumptions about which model (if any) is correct [16].

Monte Carlo gap fractions are shown in Table II. The systematic uncertainties are typically dominated by the difference in energy scale between data and Monte Carlo, but also include uncertainties from the fitting procedure. We observe that rates for harder gluon structures are far higher than supported by data, while the quark structure is in reasonable agreement with the data. The quark structure, however, has previously been shown to predict an excessive rate of diffractive W -Bosons [7].

A hard gluonic pomeron is capable of describing previous measurements [4–7], if combined with a flux factor that decreases with increasing \sqrt{s} [17]. The ratios of gap fractions shown in the lower half of Table II provide new information, since the flux factor cancels for the same \sqrt{s} , and dependence on the flux factor is reduced for different \sqrt{s} . The ratios for jets with $|\eta| > 1.6$ to jets with $|\eta| < 1.0$ show clear disagreement between the data and predictions for a hard-gluon pomeron structure, despite this cancellation. A gluon-dominated pomeron containing both soft and hard components, combined with a reduced flux factor, could describe all the data samples.

TABLE II. The measured and predicted gap fractions and their ratios.

Sample	Gap Fractions				
	Data	Hard Gluon	Flat Gluon	Soft Gluon	Quark
1800 GeV $ \eta > 1.6$	$(0.65 \pm 0.04)\%$	$(2.2 \pm 0.3)\%$	$(2.2 \pm 0.3)\%$	$(1.4 \pm 0.2)\%$	$(0.79 \pm 0.12)\%$
1800 GeV $ \eta < 1.0$	$(0.22 \pm 0.05)\%$	$(2.5 \pm 0.4)\%$	$(3.5 \pm 0.5)\%$	$(0.05 \pm 0.01)\%$	$(0.49 \pm 0.06)\%$
630 GeV $ \eta > 1.6$	$(1.19 \pm 0.08)\%$	$(3.9 \pm 0.9)\%$	$(3.1 \pm 0.8)\%$	$(1.9 \pm 0.4)\%$	$(2.2 \pm 0.5)\%$
630 GeV $ \eta < 1.0$	$(0.90 \pm 0.06)\%$	$(5.2 \pm 0.7)\%$	$(6.3 \pm 0.9)\%$	$(0.14 \pm 0.04)\%$	$(1.6 \pm 0.2)\%$
Ratios of Gap Fractions					
630/1800 $ \eta > 1.6$	1.8 ± 0.2	1.7 ± 0.4	1.4 ± 0.3	1.4 ± 0.3	2.7 ± 0.6
630/1800 $ \eta < 1.0$	4.1 ± 0.9	2.1 ± 0.4	1.8 ± 0.3	3.1 ± 1.1	3.2 ± 0.5
1800 $ \eta > 1.6/ \eta < 1.0$	3.0 ± 0.7	0.88 ± 0.18	0.64 ± 0.12	$30. \pm 8.$	1.6 ± 0.3
630 $ \eta > 1.6/ \eta < 1.0$	1.3 ± 0.1	0.75 ± 0.16	0.48 ± 0.12	$13. \pm 4.$	1.4 ± 0.3

The characteristics of the HSD events were examined using the high statistics SV trigger. We plot in Fig. 3 the distributions of the number of jets, the E_T -weighted rms jet widths, the $\Delta\phi$ between the two leading jets, and the relative ratio of diffractive to non-diffractive events as a function of the average E_T of the two leading jets, for central jets at $\sqrt{s} = 1800$ GeV. The solid lines in Fig. 3(a)–(c) correspond to the distributions for HSD candidate events ($n_{\text{CAL}} = n_{\text{L}\emptyset} = 0$), and the dashed lines show the distributions for non-diffractive events ($n_{\text{CAL}} > 0$ and $n_{\text{L}\emptyset} > 0$). These plots show that the diffractive events appear to have less overall radiation. Figure 3(d) indicates that there is little dependence of the gap fraction on average jet E_T . The MC samples (not shown) have characteristics similar to the data.

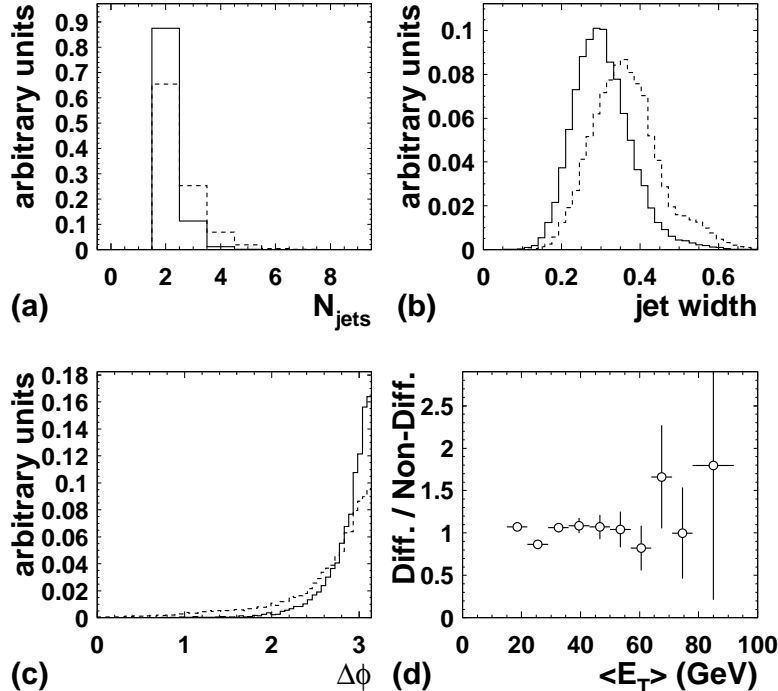


FIG. 3. Distributions of the (a) number of jets, (b) jet width, (c) $\Delta\phi$ between leading jets, for central diffractive (solid) and non-diffractive (dashed) jet events at $\sqrt{s} = 1800$ GeV. (d) The relative ratio of diffractive to non-diffractive events as a function of the average E_T of the two leading jets.

Finally, we measure the fractional momentum loss of the proton ξ , defined as [18]:

$$\xi \approx \frac{1}{\sqrt{s}} \sum_i E_{T_i} e^{\eta_i} \quad (0.1)$$

where the summation is over all observed particles. The outgoing scattered proton or antiproton (and the rapidity gap) is defined to be at positive η . Equation (1) weights heavily the well-measured central region near the rapidity gap, while particles that escape down the beam pipe at negative η give a negligible contribution. Using POMPYT events, where ξ can be determined from the momentum of the scattered proton, we have verified that Eq. (1) is reliable at both values of \sqrt{s} and for different pomeron structures. A scale factor (2.2 ± 0.3) derived from Monte Carlo is used to convert ξ measured from all particles to that from just electromagnetic calorimetric energy depositions [11]. The ξ distributions for forward and central jets at $\sqrt{s} = 630$ and 1800 GeV are displayed in Fig. 4, with the shaded region showing the variance in the distribution due to energy scale uncertainties. Energy-scale uncertainties result in a shift in ξ such that if the true distribution were below the histogram at small ξ , it would be above the histogram at large ξ .

The ξ distributions show the expected kinematic behavior of diffraction ($M = \sqrt{\xi s}$, where M is the mass of the diffractive system), peaking at larger ξ for central jets than for forward jets. Forward and central jets at $\sqrt{s} = 630$ GeV also peak at larger ξ values with respect to the corresponding distributions at $\sqrt{s} = 1800$ GeV, since for fixed diffractive mass, smaller \sqrt{s} implies larger ξ . Even though pomeron exchange is thought to dominate only

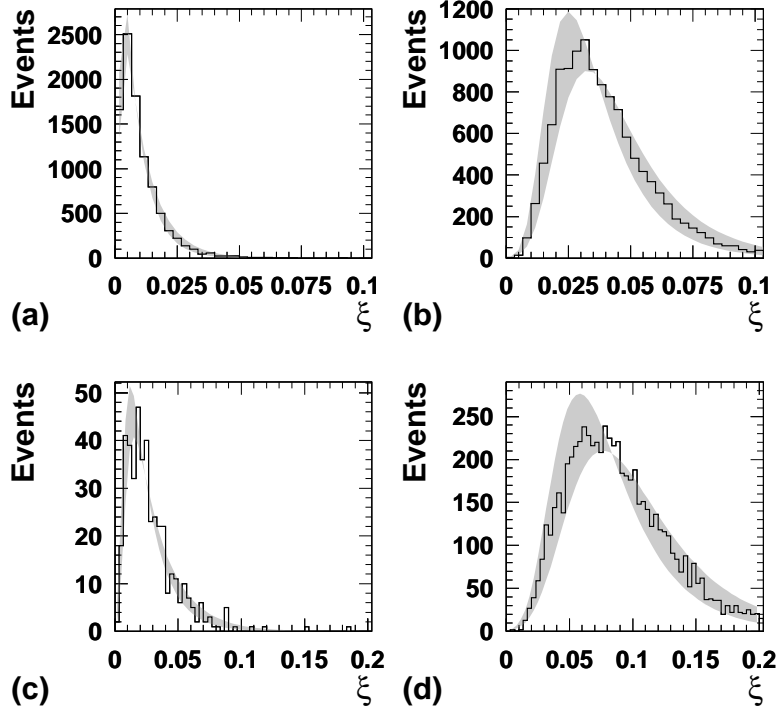


FIG. 4. The ξ distributions for $\sqrt{s} = 1800$ GeV (a) forward and (b) central jets and for $\sqrt{s} = 630$ GeV (c) forward and (d) central jets, using the SV trigger with $n_{\text{CAL}} = n_{\text{L}\emptyset} = 0$. The shaded region shows the variance in the distribution due to energy scale uncertainties (see text).

for $\xi < 0.05$, the trends of the ξ distributions can be reproduced by POMPYT. Without the observation of the scattered proton, the interpretation of these large ξ rapidity gap events is uncertain.

We have measured properties of hard single diffraction at $\sqrt{s} = 630$ and 1800 GeV with jets at forward and central rapidities. The gap fractions have been measured without applying model-dependent corrections. Within the Ingelman-Schlein model, our data can be reasonably described by a pomeron composed dominantly of quarks. For the model to describe our data as well as previous measurements, a reduced flux factor convoluted with a gluonic pomeron containing significant soft and hard components is required. We have also measured the fractional momentum lost by the scattered proton and found it greater than typically expected for pomeron exchange.

We thank the Fermilab and collaborating institution staffs for contributions to this work, and acknowledge support from the Department of Energy and National Science Foundation (USA), Commissariat à L'Énergie Atomique (France), Ministry for Science and Technology and Ministry for Atomic Energy (Russia), CAPES and CNPq (Brazil), Departments of Atomic Energy and Science and Education (India), Colciencias (Colombia), CONACyT (Mexico), Ministry of Education and KOSEF (Korea), CONICET and UBACyT (Argentina), A.P. Sloan Foundation, and the Humboldt Foundation.

REFERENCES

- [1] P.D.B. Collins, *An Introduction to Regge Theory and High Energy Physics*, Cambridge University Press, Cambridge (1977).
- [2] G. Ingelman and P. Schlein, Phys. Lett. B **152**, 256 (1985).
- [3] A. Brandt *et al.* (UA8 Collaboration), Phys. Lett. B **297**, 417 (1992).
- [4] F. Abe *et al.* (CDF Collaboration), Phys. Rev. Lett. **79**, 2636 (1997).
- [5] J. Breitweg *et al.* (ZEUS Collaboration), Eur. Phys. J. **C5**, 41 (1998) and references therein.
- [6] C. Adloff *et al.* (H1 Collaboration), Eur. Phys. J. **C6**, 421 (1999).
- [7] F. Abe *et al.* (CDF Collaboration), Phys. Rev. Lett. **78**, 2698 (1997).
- [8] L. Alvero, J.C. Collins, J. Terron and J. Whitmore, Phys. Rev. D **59**, 74022 (1999).
- [9] S. Abachi *et al.* (DØ Collaboration), Nucl. Instrum. Methods Phys. Res. A **338**, 185 (1994).
- [10] B. Abbott *et al.* (DØ Collaboration), Nucl. Instrum. Methods Phys. Res. A **424**, 352 (1999).
- [11] K. Mauritz, Ph.D. Dissertation, Iowa State University, 1999 (unpublished).
- [12] B. Abbott *et al.* (DØ Collaboration), Phys. Rev. Lett. **82**, 2451 (1999).
- [13] P. Bruni and G. Ingelman, DESY 93-187, 1993 (unpublished). We used a modified version of 2.6.
- [14] H.-U. Bengtsson and T. Sjöstrand, Comp. Phys. Comm. **46**, 43 (1987); T. Sjöstrand, CERN-TH.6488/92. We used version 5.7.
- [15] A. Donnachie and P.V. Landshoff, Nucl. Phys. B **303**, 634 (1988).
- [16] Ref. [4] obtained a gap fraction of $(0.75 \pm 0.10)\%$ assuming a hard gluon structure. If we correct our corresponding measurement of $(0.65 \pm 0.04)\%$ in a comparable manner, we obtain a consistent value of $(0.88 \pm 0.05)\%$.
- [17] K. Goulianos, Phys. Lett. B **358**, 379 (1995).
- [18] J. Collins, hep-ph/9705393, 1997 (unpublished).